

# Stick to slip transition and adhesion of lubricated surfaces in moving contact

Günter Reiter, A. Levent Demirel, John Peanasky, Lenore L. Cai, and Steve Granick  
*Materials Research Laboratory and Department of Materials Science and Engineering,  
University of Illinois, Urbana, Illinois 61801*

(Received 1 February 1994; accepted 12 April 1994)

The friction of dry self-assembled monolayers, chemically attached to a solid surface and comprising a well-defined interface for sliding, is compared to the case of two solids separated by an ultrathin confined liquid. The monolayers were condensed octadecyltriethoxysilane (OTE). The liquid was squalane ( $C_{30}H_{62}$ ), a film 2.0 nm thick confined between parallel plates of mica. The method of measurement was a surface forces apparatus, modified for oscillatory shear. The principal observations were the same in both cases: (1) Predominantly elastic behavior in the linear response state was followed by a discontinuous transition to a mostly dissipative state at larger deformations. The elastic energy stored at the transition was low, of the order of 0.1 kT per molecule. This transition was exactly repeatable in repetitive cycles of oscillation and reversible with pronounced hysteresis. (2) The dissipative stress in the sliding state was almost independent of peak sliding velocity when this was changed over several decades. Significant (although smaller) elastic stress also persisted, which decreased with increasing deflection amplitude but was almost independent of oscillation frequency. (3) The adhesive energy in the sliding state was significantly reduced from that measured at rest. This similarity of friction in the two systems, dry and wet sliding, leads us to speculate that, similar to plastic deformation of solids, sliding in the confined liquid films is the result of slippage along an interface.

## I. INTRODUCTION

When a solid body is moved over a solid surface most of the energy needed for this process cannot be regained and is wasted in this endeavor. The origin of this dissipation of energy is attributed to friction. However, a detailed explanation of the molecular processes involved in friction is still lacking.<sup>1-4</sup> Several attempts were made to relate to roughness (see, e.g., Ref. 3). To overcome an asperity the sliding body has to be lifted or the asperity has to be deformed. For metal-metal contacts that usually form rough interfaces this idea certainly has some validity. However, experiments with molecularly smooth surfaces showed that roughness is not the only source of friction. In some sense analogous to the above idea, explanations based on the adhesion between the bodies were developed. For example, in the "cobblestone model"<sup>5-7</sup> frictional loss is related to the strength of adhesion. Experiments with Langmuir-Blodgett layers of hydrocarbon and fluorinated molecules, however, contradict such a relation.<sup>8,9</sup> Although the fluorinated molecules adhere less they exhibit a significantly higher friction. For the case of crystalline surfaces like graphite<sup>10</sup> sliding past each other, elaborate atomistic models were developed<sup>11-16</sup> where energy is dissipated by exciting vibrational modes.

Soon it was recognized that the addition of a thin lubricating layer in between the two solids can reduce friction (see, e.g., Ref. 4). Unfortunately, only little is known about what is happening to the lubricant layer that can be as thin as one molecular layer. Even if the lubricant is a liquid, in such a confined geometry it might behave solid-like. Computer simulations of confined molecules as used in boundary lubrication indicate that the energy is lost due to the transition from a solid-like to a liquid-like state of the lubricant

layer.<sup>17-19</sup> Simulations for a rather densely packed adsorbate layer that is exposed to shear show that this transition is abrupt and hysteretic.<sup>11</sup>

A burgeoning experimental literature is exploring the molecular aspects of friction as solids slide over one another. In this endeavor the separation of asperity-asperity contact of rough surfaces from other fundamental issues is critical and many early studies employed the surface forces apparatus.<sup>20-29</sup> More recently the friction force microscope was employed to study friction with a high lateral resolution.<sup>9,30</sup> Quartz crystal microbalance studies are also able to provide information about friction on an atomic level.<sup>31,32</sup> Investigations on Langmuir-Blodgett films show a correlation between adhesion hysteresis and friction.<sup>26,33</sup>

In the present study our main interest focused on the startup of sliding and the transition from a solid-like state to the sliding state. The following questions are addressed: What is happening to such a film of confined molecules when sliding starts and does this affect adhesion? Where is the slip occurring? What is the effect of sliding velocity? How is energy dissipated in the sliding state? We expand on a previous communication.<sup>34</sup>

For this purpose we compared two systems. In one case we fixed the molecules by chemical attachment at the mica surfaces and thereby predefined where the slip would happen. The second system was a liquid in the bulk. The applied oscillatory shear experiments differ physically from steady-state sliding in the same direction because the deflection amplitude was much smaller than the contact diameter. Therefore we always looked at the same molecules in the gap, which were equilibrated to the conditions of confinement.

The response described below was highly regular. This contrasts with the noise and fluctuation that characterize

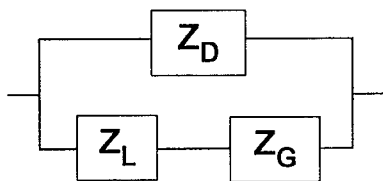


FIG. 1. Sketch of the mechanical model used to analyze the data. Contributions from the device and a serial combination of glue layers and liquid are in parallel. The symbols  $Z_D$ ,  $Z_G$ , and  $Z_L$  are the complex impedances of the device, glue layers, and liquid, respectively. As described in Ref. 35, the complex impedance of each element can be represented by a parallel arrangement of elastic and dissipative subelements.

much friction response in systems of an engineering nature. We believe this difference to be a consequence of the smoothness of the mica surfaces, the averaging over large enough areas, and the fact that the molecules had enough time to adjust to confinement and shear conditions.

## II. EXPERIMENT

### A. Apparatus

The measurements were done with a surface forces apparatus modified for oscillatory shear measurements, as is described in detail in Refs. 28 and 35. In brief, two atomically smooth mica sheets are glued onto cylindrically shaped glass lenses. These sheets are brought together with subnanometer accuracy. Due to elastic deformation, mostly of the underlying glue layers, the actual point of contact of the mica surfaces is flattened. One can consider the geometry of the contact area as two parallel plates. The diameter of the flattened area under small loads is of the order of  $10\ \mu\text{m}$ . In a typical experiment the surfaces of the mica sheets are separated only by a few nanometers. Thus the molecules are confined in a thin channel which is orders of magnitude wider than it is thick. Multiple beam interferometry with a resolution of about  $0.2\ \text{nm}$  is used to measure the distance between the mica surfaces.

The top lens is attached onto a shear device consisting of two piezoelectric bimorph assemblies. One acts to apply force, the other to sense resulting deflection. As the device operates, there is some compliance in the device itself and some in the sample of interest. This serial combination, in parallel with the complex impedance of the bimorphs themselves, constitutes the mechanical circuit by which we model the device. The mechanical circuit is sketched in Fig. 1.

In this model, the force applied to this parallel combination is split according to the ratio of the complex impedance. Here  $Z = k + i\omega b$ ,  $k$  is the real part of  $Z$ , the spring constant,  $\omega$  is radian frequency, and  $b$  is the (dissipative) dashpot coefficient. Denoting applied force by the symbol  $F$ , this gives

$$F = (|Z_D + Z_S|)\Delta x_{\text{tot}}, \quad (1)$$

where  $Z_D$  and  $Z_S$  are the complex impedances for the device (mainly represented by the bimorphs) and the serial combination of glue and sample, respectively, and  $\Delta x_{\text{tot}}$  is the total deflection of the receiver bimorph, equal to the deflection of the series combination of glue and confined liquid.

The observed deflection in the case of an extremely stiff sample as determined by bringing top and bottom dry mica surface in direct contact is attributed to deformation of the glue between mica sheet and glass lens. The deformability of the glue in series with the confined liquid film is accounted for by

$$\Delta x_L = \Delta x_{\text{tot}}(|Z_G/(Z_G + Z_L)|). \quad (2)$$

Here  $\Delta x_L$  is the actual deflection within the confined liquid film and  $Z_G$  and  $Z_L$  are the complex impedances representing the glue layers and the confined liquid, respectively.

This analysis allows one to correct the raw data for apparatus compliance. Because of the parallel arrangement of the device, the force applied to the system (device, liquid, and glue) is not the same as the force applied to the confined liquid film. In particular, the quantity we denote as “applied stress” (applied to the parallel combination of  $Z_D$  and  $Z_S$ ) exceeds the quantity we denote as “acting stress” (representing the part of the applied stress acting on the confined liquid film). Acting stress is balanced by the responding stresses generated within the confined liquid film.

### B. Samples

For the present study we looked at two different systems. The case of two opposing solid surfaces was represented by mica sheets coated with self-assembled monolayers of condensed octadecyltriethoxysilane (OTE) molecules. The preparation process is described in Ref. 36. The molecules were densely packed, fixed with their heads to mica, and their methyl-terminated tails pointing away from the mica surface. The thickness of two such monolayers, brought into van der Waals contact in the surface forces apparatus, was  $5.1 \pm 0.3\ \text{nm}$ .<sup>37</sup> One should not think of these layers as perfect single crystals. Though there are certainly ordered regions, such self-assembled monolayers are expected to have a significant amount of dislocations and defects. Recent AFM investigations on similar systems support this assumption.<sup>38</sup> It has to be noted that the heads of the molecules were permanently fixed at the mica surface and consequently were not able to change their position on the mica surface. The only motion these molecules could experience was some bending and tilting of the tails. Consequently, as one surface slid past the other, the point of slip was well defined.

To study the case of an ultrathin lubricant, squalane was placed between two crystalline mica surfaces. Squalane ( $\text{C}_{30}\text{H}_{62}$ ), a branched alkane with six methyl sidegroups, is well-known as a model lubricant. Probably due to its irregular structure, squalane showed no oscillatory surface forces when the two mica sheets were brought together, but one sole attractive minimum at approximately  $2.2\ \text{nm}$ , followed by repulsion so steep that increased load resulted in no perceptible change in the film thickness. This presented the great advantage that measurements at various applied loads were actually performed at almost the same thickness of the squalane film.

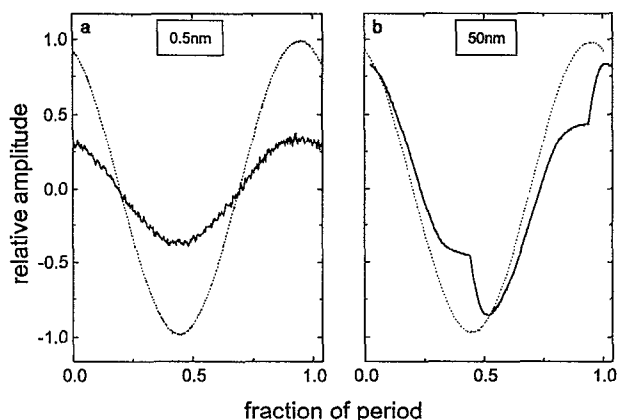


FIG. 2. Typical response to (a) small (0.5 nm) and (b) large (50 nm) effective deflection amplitude. The system is a 2.0 nm thick squalane film at about 1 MPa normal pressure. The frequency of oscillation is 0.13 Hz. The dotted line represents the calibration response of the shear device without contact to the lower surface. The full line shows the actual response of the confined liquid including the device contribution. The noise in (a) originates mainly from vibrations in the laboratory.

### III. RESULTS

#### A. Raw data

In all the investigations presented below we applied a sinusoidally varying force  $F(t)$ :

$$F(t) = F_0 \sin(\omega_1 t), \quad (3)$$

where  $\omega_1 = 2\pi\nu_1$  is the radian frequency of the shear oscillation,  $t$  indicates time, and  $F_0$  the force amplitude. The frequency  $\nu_1$  was varied between 0.05 and 260 Hz. The responding signal, as detected by the receiver bimorph, was recorded with a digital oscilloscope. Usually many periods were added and averaged to increase the signal-to-noise ratio. As long as the deformation of the film was small the response was sinusoidal, but attenuated and slightly retarded compared to the input [Fig. 2(a)]

$$x(t) = x_0 \sin(\omega_1 t - \phi). \quad (4)$$

$x(t)$  is the deflection,  $x_0$  the deflection amplitude, and  $\phi$  is the phase shift with respect to the input signal. This was a predominantly elastic response (discussed below). When the deformation amplitude exceeded a critical level, the response became distorted [Fig. 2(b)]. One can clearly see how the increase in deflection slowed down and accelerated again once a certain point was reached. This distortion was reproducible and occurred exactly at the same position during every period.

Four periods of a typical signal (0.13 Hz and 60 nm amplitude of deflection, for a 2.0 nm thick squalane film at about 1 MPa normal pressure) are shown in Fig. 3 (solid line). The dotted line shows the best fit of a sinusoidal wave at the input frequency to the data. The dash-dotted line gives the difference between fit and measured data. It should be emphasized that adding many hundred periods did not smear out the distortion. In that sense this distorted waveform represents an intrinsic response of the confined liquid. It is thus not surprising that the Fourier transform of such extremely

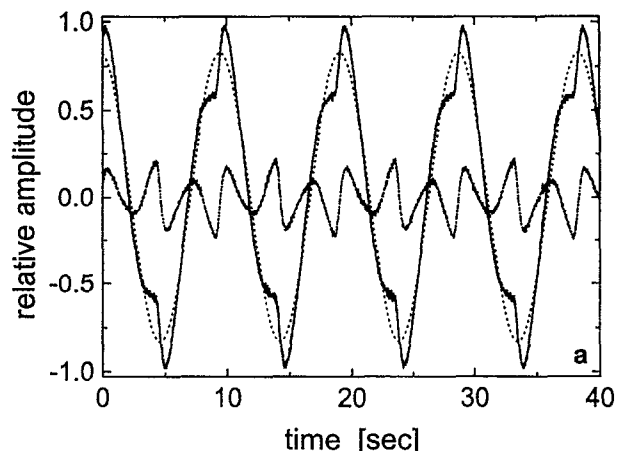


FIG. 3. Characteristic response of a 2.0 nm thick squalane film at about 1 MPa normal pressure sheared at 0.13 Hz with an amplitude of about 60 nm which is large enough to be in the sliding regime. The solid line shows the deflection as a function of time for four periods. Note the regularity of the pattern. The dotted line represents the fundamental component of the signal as determined from the Fourier transform of the data. The dashed-dotted line gives the difference between the solid and the dotted line.

periodic signals gave a spectrum of contributions at discrete frequencies. A series of odd higher harmonics was obtained:

$$x(t) = \sum_k [A_k \sin(\omega_k t - \phi_k)], \quad k = 1, 3, 5, 7, \dots, \quad (5)$$

$$\omega_k = k\omega_1. \quad (6)$$

Here  $A_k$  are the amplitudes of the harmonic components.

Figure 4 gives an example for the Fourier transform of such a periodic signal. The number of harmonics which could be resolved depended partly on the background (mostly determined by mechanical vibrations and noise in the laboratory), but also on deflection amplitude and fre-

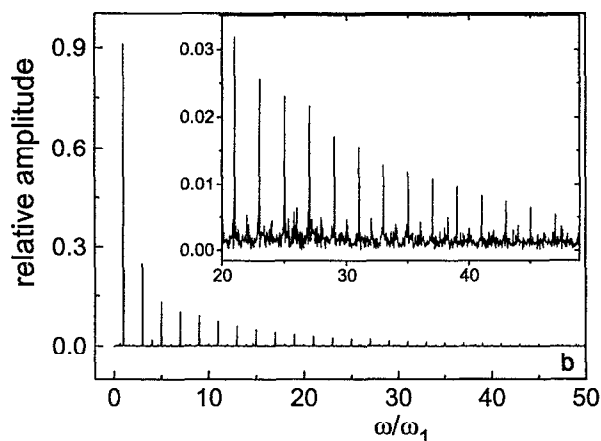


FIG. 4. Fourier transform of a distorted waveform for the same conditions as in Fig. 3 but for an amplitude of about 10 nm. The radial frequency  $\omega$  is normalized by the input frequency  $\omega_1$ . The inset amplifies the range from 20 to 50 in  $\omega/\omega_1$ . The amplitudes are normalized by the amplitude of the calibration signal. For very low noise conditions like in this example harmonics higher than 50 could be resolved. No correction for device contributions was made.

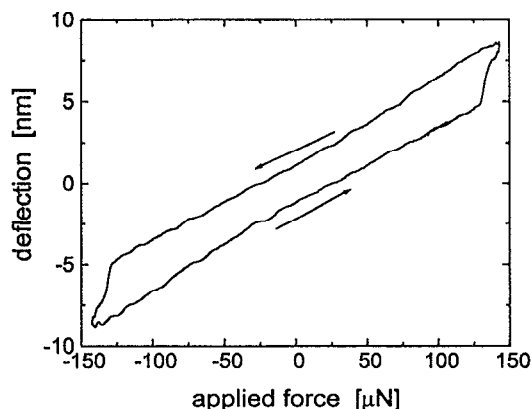


FIG. 5. Lissajous representation (deflection as a function of applied force) of the response of squalane (2.0 nm, approximately 1 MPa normal pressure) in the sliding regime: data were taken at 1.3 Hz. The data are not corrected for the device compliance.

quency. Especially at the lowest frequencies the distortion of the responding signal (deviation from a pure sinusoidal wave) resembled very much the patterns of stick-slip motion in experiments where the driving block is moving steadily.<sup>39</sup>

An alternative way to represent such data is a stress-strain pattern. In Fig. 5 we plot applied force vs resulting amplitude during a cycle of oscillation at 1.3 Hz. One can clearly observe the start of sliding shortly before the maximum force was reached. However, due to the finite time resolution of the detection system this slip is smeared out a little. In the discussion below we do not pursue this analysis because it is not yet clear, in this approach, how to correct for the apparatus compliance. The data in Fig. 5 are not corrected for the contribution of the glue layers, in which a significant part of the deformation occurred.

Though similar nonlinear responses were observed in several other systems<sup>40–42</sup> there exists to date no unique theoretical way to analyze nonlinear responses or to interpret the physical meaning of higher harmonics as in Fig. 4. Although in some cases it is possible to relate the amplitude and phase values of the higher order terms to higher nonlinear moduli,<sup>40,41,43</sup> the physical meaning of such moduli is unclear in cases of evident stick-slip as in the present systems. For the interpretation of the results at the present time we concentrate on the response at the fundamental frequency. Such a simplification seems to be partially justified by the fact that the dissipated energy is completely determined by the fundamental component alone.<sup>40,41</sup> The alternative analysis in terms of a force-deflection cycle, as in Fig. 5, will be presented elsewhere.

## B. Linear response

Below a certain maximum acting stress  $\sigma_0$  (defined by the amplitude of the sinusoidal force acting on the film only, normalized by the area of contact) the response of both systems was found to be highly elastic as can be seen in Fig. 6. The stress was applied in a sinusoidal fashion at a frequency of 1.3 Hz. In this linear response regime the resulting deflection indicated the resulting stress within the sample. This was

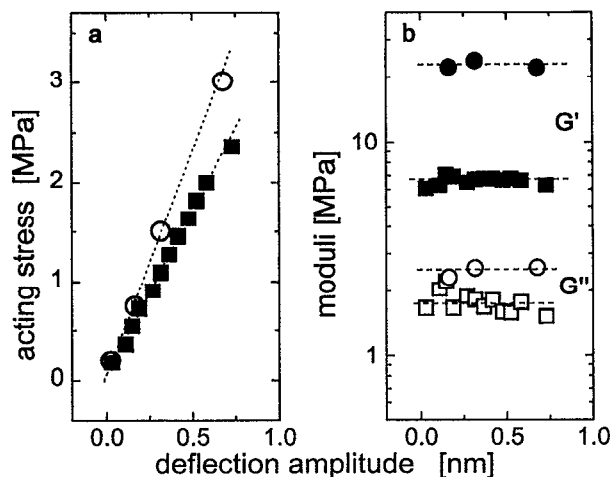


FIG. 6. Response at small deflections. (a) Stress acting on the confined molecules vs the resulting deflection of the top surface for OTE (open circles) and squalane (solid squares). OTE layers were 2.5 nm thick and the molecules chemically attached onto the mica surfaces. There was zero normal pressure applied. The squalane film was 2 nm thick and about 1 MPa normal pressure was applied. Data were taken at 1.3 Hz in the direction of increasing stress. (b) Storage modulus  $G'$  (solid symbols) and loss modulus  $G''$  (open symbols) for the data shown in (a). Circles are for OTE and squares for squalane. Data are corrected for device compliance.

resolved into in-phase and out-of-phase components.<sup>44</sup> The contribution that was in phase with the driving stress, normalized by the ratio of deflection over film thickness,<sup>45</sup> gave the inverse elastic shear compliance  $J'$ , which we represented here as an elastic shear modulus  $G'$  (see Ref. 44 for discussion of the difference between compliance and modulus). The loss modulus  $G''$  was determined in an analogous way from the out-of-phase response. With increasing deflection these moduli were constant within the error bars of the measurement, indicating that deflections up to approximately 1 nm did not disturb the structure of the confined molecules significantly.

In this linear regime the responding stress was a purely sinusoidal function. In Fig. 6 one notes that  $G' \approx 10G''$ , indicating a predominantly elastic response. It has to be noted that for both systems there existed attraction between the top and the bottom surfaces, mostly van der Waals interactions. In the case of squalane we also applied external normal pressure of about 1 MPa. Repeating this experiment at different frequencies showed (within the experimental frequency window of 0.05–200 Hz) no significant change in the storage and loss moduli,<sup>46</sup>  $G'$  being much larger than  $G''$  in all cases.

In earlier studies<sup>21,24,28,29</sup> liquid films with much lower (mostly undetectably low) elastic moduli were investigated. Such behavior was the result of slightly thicker or less compressed liquid films. In those cases increasing the deflection amplitude led from a linear regime to highly nonlinear shear thinning regime. Preliminary results suggest that there exists a gradual transition from the rather liquid-like case to the solid-like case of the present study by increasing the applied normal pressure on the system. One may say that the results presented here describe the case of rather extreme confinement.

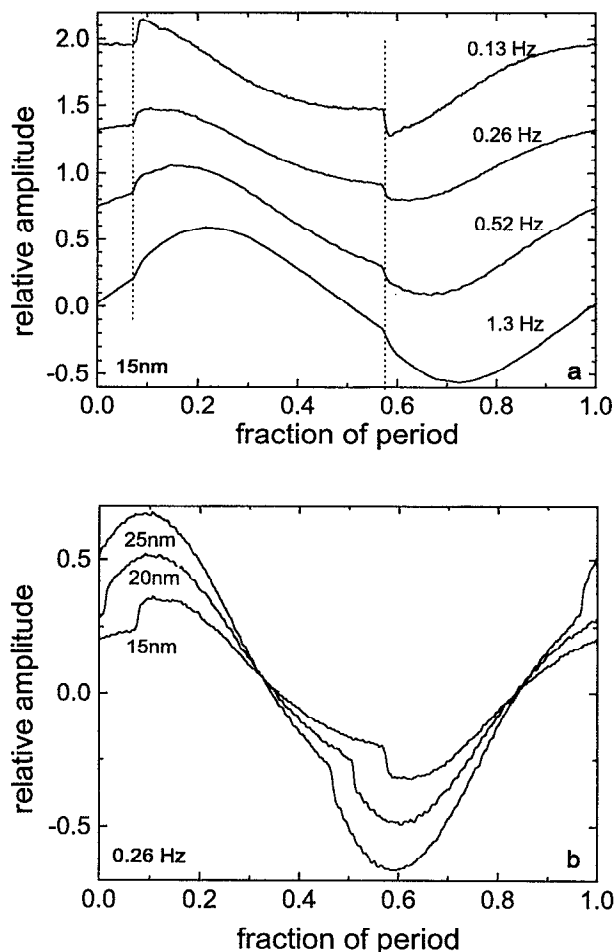


FIG. 7. Raw traces showing the characteristic response at large deflection amplitudes for squalane (2.0 nm, approximately 1 MPa normal pressure). Deflection is plotted vs the fraction of a period. (a) Constant amplitude (15 nm for out-of-contact) and frequencies from 0.13 to 1.3 Hz. The curves are shifted for clarity. The perpendicular dotted lines connect the points of slip for the various frequencies indicating constant acting stress at these points. (b) Constant frequency 0.26 Hz and three different amplitudes (the indicated oscillation amplitudes are for free oscillation in air).

### C. Stick to slip transition

The linear response at small deformations (presented in Fig. 6) of the OTE and squalane systems differed in magnitude but not qualitatively. Probing for the maximum elastic deformability, the acting stress  $\sigma_0$  was increased further. At a well defined point,  $\sigma_0 = \sigma_{0,crit}$ , the response of the system changed abruptly and drastically.<sup>47</sup> At low values of  $\sigma_0$  the response was mostly attenuated but sinusoidal as already noted. However, exceeding  $\sigma_{0,crit}$  led to a highly distorted response. From the raw signals we observed very characteristic trends if we varied frequency or amplitude of the acting stress oscillation.

By varying the frequency of the applied force, at constant amplitude, it emerged that the responding waveform showed a kink at the same fraction of the period of the oscillation, regardless of frequency [Fig. 7(a)]. This means that the kink (interpreted below as a point of slip) is determined by the same applied stress. At constant frequency, however,

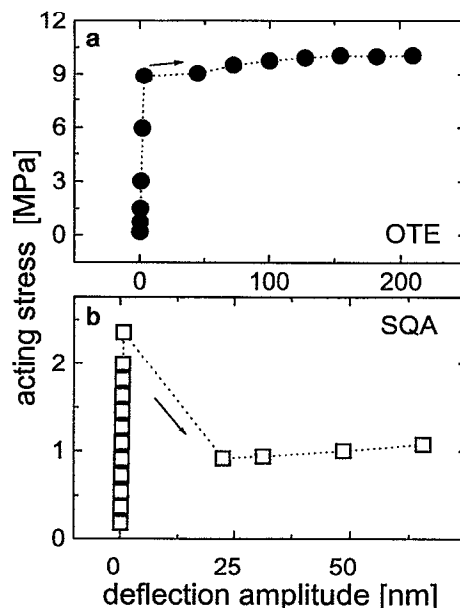


FIG. 8. Stress acting on the confined molecules vs the deflection amplitude of the top surface for (a) OTE (zero normal pressure) and (b) squalane (2.0 nm, approximately 1 MPa normal pressure). The data were taken at 1.3 Hz in the direction of increasing deflection amplitude.

increasing the applied stress led to a shift of the “indentation” towards earlier times [Fig. 7(b)]. Interestingly, the applied stress at the time of the indentation was almost the same.

Similarly, a discontinuous transition was observed for the amplitude of the responding oscillatory deflection of the top surface as the applied stress was raised (Fig. 8). Up to  $\sigma_{0,crit}$  (linear response), the sample was stiff. At  $\sigma_{0,crit}$  the sample weakened and a given peak stress (during oscillation) induced greater peak deflection. For OTE the peak stress was nearly independent of peak deflection. For squalane it actually dropped below  $\sigma_{0,crit}$ . At this point it should be mentioned that in this sliding regime the design of our apparatus does not allow the deflection amplitude to increase beyond the amplitude one would get for the same applied stress of the shear attachment swinging free in air. Therefore there is no paradox in the finding that peak deflection, in the sliding regime, was nearly independent of peak stress.

Only the response at the fundamental frequency of the stress is considered below. Figure 9 shows elastic and dissipative stresses vs deflection amplitude and again the remarkably similar behavior of the two systems under investigation. At  $x_{0,crit}$  we observed an abrupt change from a highly elastic response to a mostly dissipative state. It has to be emphasized that in this sliding state *both* contributions, elastic and dissipative, were rather independent of the amplitude of deflection. This is remarkable as one might expect that the independence of acting stress on deflection amplitude might arise from a compensation of an increasing dissipative and a decreasing elastic stress.

Up to this point, we presented data taken in the direction of increasing amplitude of oscillation only. Reversing the direction unveiled remarkable hysteresis. An example is

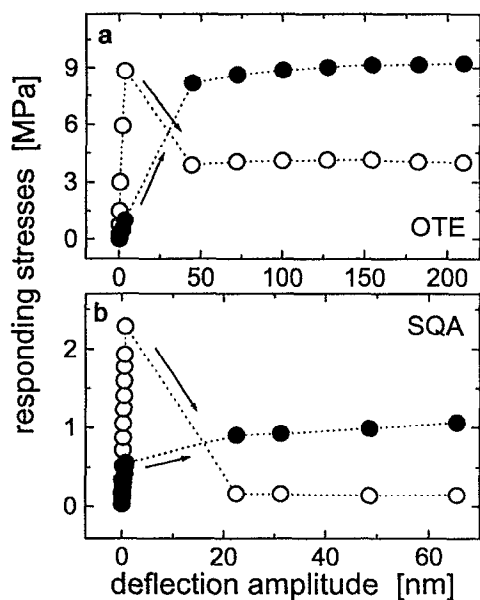


FIG. 9. Responding elastic (open circles) and dissipative (solid circles) stresses which balance the acting stress for the data in Fig. 8. (a) OTE and (b) squalane. This analysis only considers the contribution at the fundamental frequency.

shown in Fig. 10 for squalane. Similar behavior was found for the OTE system. Without reverting to the highly elastic linear response, it was possible to go to lower amplitudes of deflection than were accessible in the direction of increasing stress. The minimum deflection that could be reached in this understressed state depended sensitively on the noise level in the laboratory. Slight vibrations could lead to a switch from

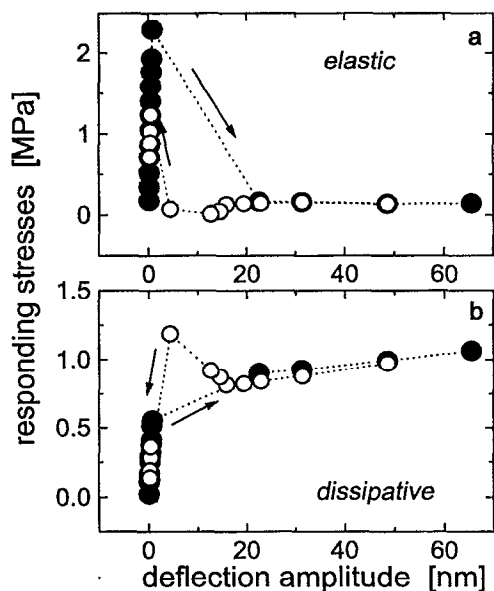


FIG. 10. Responding elastic (a) and dissipative (b) stress vs deflection amplitude for the data of Fig. 9(b) (solid circles), now including data in the direction of decreasing deflection amplitude (open circles). Note the pronounced hysteresis.

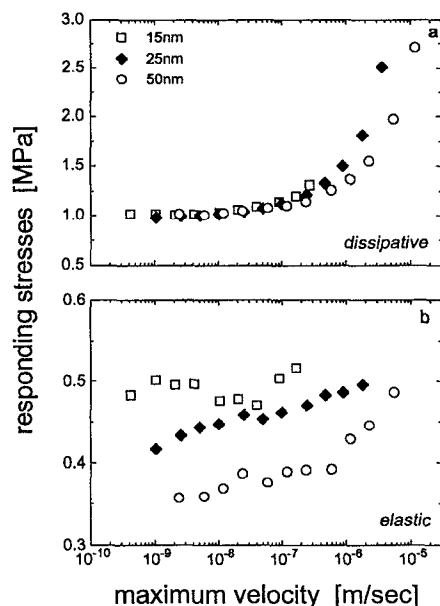


FIG. 11. Responding dissipative (a) and elastic (b) stress vs the maximum velocity ( $v_0 = \text{deflection amplitude} \times \text{radian frequency}$ ) of the top surface. Note that  $v_0$  is plotted on a logarithmic scale. The data are for a squalane film of 2.1 nm and at a normal pressure of about 1 MPa. The frequency was varied between 0.05 and 130 Hz for each amplitude. The indicated amplitudes are for free oscillation in air.

the dissipative to the elastic state. In most cases the results from the increasing and the decreasing stress direction did not exactly superpose. We interpret this to indicate some irreversible or extremely slowly reversible changes induced by shearing the system at high amplitudes.

#### D. Steady-state response in the sliding regime

Experiments on squalane in the sliding state, with the frequency increased but the amplitude constant, are shown in Fig. 11. The data are plotted vs the maximum velocity  $v_0$  ( $v_0 = 2\pi\nu_1 x_0$ ) of the top surface. One can see that in this state the response of the system was actually velocity-dependent. This contrasts strongly with the response below  $x_{0,\text{crit}}$ , which depended on deflection amplitude but not frequency. At the highest peak velocities the dissipative part increased sharply whereas the elastic contribution was not so much velocity-dependent and rather decreased as the amplitude of deflection is raised.

For squalane one thus can identify three regimes. First, almost no movement of the top surface up to large stresses. Second, after an abrupt transition, a regime where the deflection of the top surface increased without a notable increase of the driving stress. Third, to move the top surface even faster, the driving stress had to be increased again.

#### E. Normal load—Squalane

We looked also at the dependence of our results on the normal load (denoted by  $L$ ) on the film. In Fig. 12 the acting shear force for squalane, and in Fig. 13 the responding shear force, are plotted vs normal load. In this particular case the top surface oscillated at a frequency of 1.3 Hz and an initial

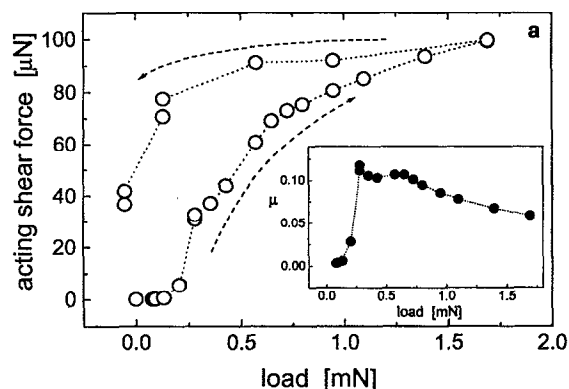


FIG. 12. Influence of normal load on the force required to shear squalane. The top surface is oscillating at 1.3 Hz and 10 nm ("free" oscillation) while the normal load was increased. The film thickness is varying between 2.2 and 1.9 nm at the lowest and highest loads, respectively. Acting shear force as a function of normal load for increasing and decreasing load. The inset shows the ratio of force divided by load (=friction coefficient  $\mu$ ) for the increasing load direction.

amplitude of about 10 nm as the normal load was increased. Each point was averaged for about 5 min. (The data are plotted as force vs load, not normalized by area to give stress, to eliminate uncertainties of the contact area measurements.) Up to a load of about 0.2 mN the shear force was rather low. The increase in the shear force then slowed down.

An equivalent way to express this is in terms of a friction coefficient,  $\mu = F/L$  (see Ref. 48). After an initial period where  $\mu$  (shown in the inset of Fig. 12) increased to about 0.1,  $\mu$  decreased slightly at higher loads.

The dissipative force was always larger than the elastic force. Reducing the load resulted in a pronounced hysteresis. Negative load had to be applied in order to move the two mica surfaces apart. It has to be noted that the separation of the mica surfaces did not change by more than about 0.3 nm between the most compressed state and the point from which they jumped apart. Part of the hysteresis might be due to kinetic effects, as 5 min per datum might not be enough for equilibration. Incidentally we also note that the surface force,

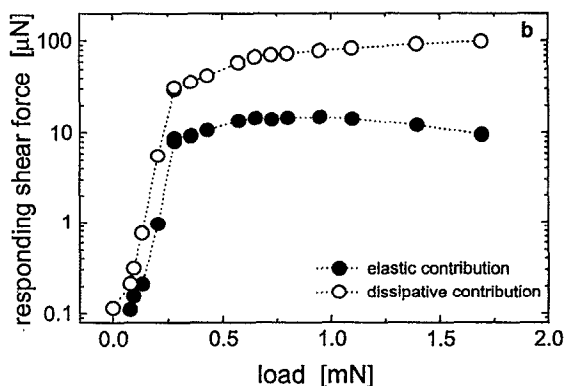


FIG. 13. Responding elastic (solid circles) and dissipative (open circles) force for the same data as in Fig. 12 in the direction of increasing load. Note that the shear force is plotted on a logarithmic scale.

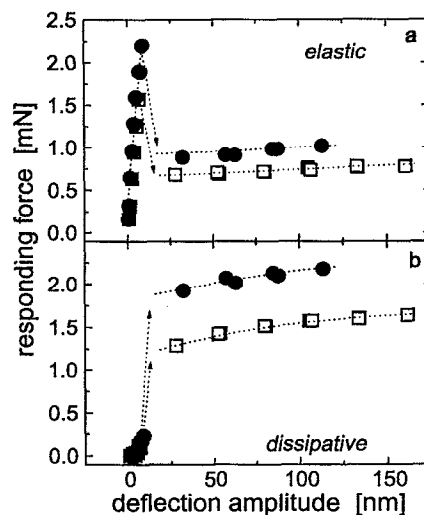


FIG. 14. Elastic and dissipative responding force for OTE monolayers at zero (open squares) and 2 mN (solid circles) load as a function of deflection amplitude. The data were taken at 1.3 Hz. The contact area is approximately  $400 \pm 100 \mu\text{m}^2$ . Within the resolution the area does not change.

i.e., the adhesive force which resisted separation of the surfaces, between the two mica plates appeared to lessen under shear. A detailed study of the effects of shear on the measured interaction between the two mica plates is planned for the future.

## F. Normal load—OTE

The effect of increasing load on the transition between the elastic and dissipative (sliding) state is illustrated in Fig. 14 for OTE. Qualitatively the behavior for zero load and a load of 2 mN was similar. Quantitative differences, however, existed for the levels of the force  $F_{0,\text{crit}}$  necessary to start sliding and the values of elastic and dissipative force above  $F_{0,\text{crit}}$ . At a load of 2 mN, these forces were larger by about 50% than at zero normal load.

In this calculation, note that the diameter of the contact can be measured with an accuracy of  $\pm 5 \mu\text{m}$ . At zero load the contact spot for OTE had a diameter of  $20 \pm 5 \mu\text{m}$  and did not measurably change at a load of 2 mN. (Squalane at 1 MPa showed a diameter of  $10 \pm 5 \mu\text{m}$ .) The resolution of the measurements of the contact diameter was therefore insufficient to decide if the change in the response of the monolayers to shear could be completely attributed to an increase in the contact area. Similar effects have been observed also for squalane.

## G. Adhesion during slip

Finally, we measured the adhesive force (to separate the two OTE layers) as a function of deflection amplitude at zero load. This pull-off force was normalized by  $3\pi R$ , where  $R$  is the mean radius of curvature of the cylindrical glass lenses. According to JKR theory<sup>49</sup> this gives the adhesive energy. Without shear we measured  $22 \text{ mJ/m}^2$ , in agreement with previous measurements from this laboratory,<sup>36,37</sup> and the results under shearing conditions are normalized by that value.

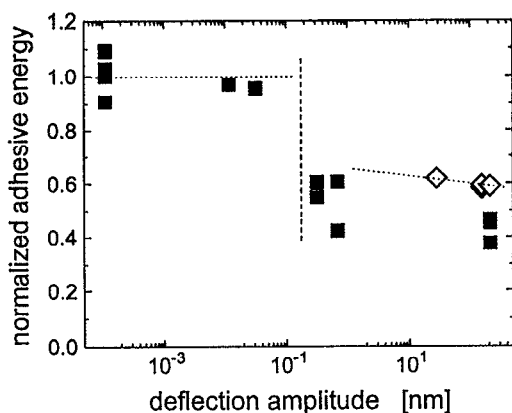


FIG. 15. Normalized adhesive energy as a function of deflection amplitude (at zero normal load) for two OTE monolayers in contact. The filled squares are determined by shearing at a constant amplitude (1.3 Hz) and pulling the surfaces apart using a mechanical motor. The open diamonds result from measurements under constant negative load and increasing the shear amplitude (with a piezoelectric device that introduced less vibrations than the mechanical motor) until the surfaces separate. The dotted lines are guides for the eye, taking into account the effect of vibrations and noise. The dashed line separates the highly elastic regime from the sliding regime.

The effect of shear was investigated in two ways. We either applied a certain shear and separated the samples while shearing, or we applied a negative load at zero shear and afterwards increased the shear amplitude at 1.3 Hz until the surfaces jumped apart.

As can be seen in Fig. 15, jumps apart were indeed induced by shear. A reduction of the pull-off force was found when a negative load of about 60% of the pull-off force measured without shear was applied and the shear amplitude was gradually increased. At an amplitude of some 10 nm the surfaces suddenly jumped apart and the adhesion energy as determined from the pull-off force was reduced by about 40%. As no movement of motors is needed for this type of measurement the contribution of mechanical noise is significantly lower than in the case of separating while shearing. This is a direct proof that the effective adhesive energy is influenced by shear.

Similar measurements were attempted for squalane but were unsuccessful because the adhesive energy is lower (about 2 mJ/m<sup>2</sup>). Therefore the effects we were interested in were buried within the scatter of the measurements.

#### IV. DISCUSSION AND CONCLUSIONS

The surprising similarities between the two distinctly different systems, OTE (chemically attached) and squalane (liquid in the bulk), lead us to look for a common explanation of the observed effects. The purpose of using grafted molecules (OTE) was to predefine the plane of slip. On the other hand, we tried to keep the two systems as comparable as possible. As seen in Fig. 6, the viscoelastic response at small deformations was very similar. Both systems showed solid-like behavior with storage moduli of similar magnitude. Solid-like behavior is less surprising for OTE monolayers. Incidentally, it has to be emphasized that the value found for  $G'$  indicates that the molecules are not in a crystalline

order, at least not all of them. For a crystalline state we would expect a much higher value for  $G'$ . The picture we have in mind is a locally ordered system with many defects (grain boundaries between ordered domains) similar to Bragg's well-known bubble model for a two-dimensional system.<sup>50</sup> Accordingly the CH<sub>3</sub> ends have some flexibility and the movement is only correlated within ordered domains and mostly independent between domains. In this view the low shear elasticity of OTE is not surprising.

The 2.0 nm thick squalane film at about 1 MPa normal pressure also showed solid-like behavior, which we attribute to confinement of the molecules between rigid solid surfaces. Earlier studies indicate that slightly thicker or less compressed liquid films show much lower elastic moduli.<sup>21,24,28,29</sup> In the present experiments the results describe the case of rather extreme confinement. At present it is unclear how the molecules fill the channel between the mica surfaces. Computer simulations indicate that shorter linear alkanes under such confinement tend to orient with their long axis parallel to the surface.<sup>51,52</sup> This leads to an oscillatory surface force-distance profile at small separations of the mica surfaces. Squalane did not show oscillations in the surface force. A single attractive minimum around  $2.2 \pm 0.2$  nm was found as will be reported in detail elsewhere. Concerning the structure of the molecules one might speculate that these molecules are coiling up and have a rather globular shape with a diameter of about 1.0 nm. This would mean that at about 2.0 nm we were left with a monolayer of these molecules at each mica surface.

Both systems behaved like "soft" solids at low deformations at frequencies between 0.05 and 260 Hz. The level of elasticity is about three orders of magnitude less than would be typical of a crystal in the bulk.<sup>44</sup> In addition, one observes that  $G'$  and  $G''$  were constant up to deflections amounting to a large fraction of the film thickness, again in contrast to a crystal or glass in the bulk. With increasing applied stress one has to expect a breakdown of this elastic behavior. No solid material can be deformed elastically beyond a certain limit. At a high enough stress it will yield. The surprising fact is that such yielding for our systems was found to be extremely well defined and repeatable in repetitive cycles of oscillation. Exactly the same rupture response (shape of the distorted waveform) was found even after many periods had passed. The lack of irregularity of the signal and the sharpness of the transition together with the hysteretic behavior and the existence of a metastable region are analogous to features of a first-order phase transition. However, in the present case we are dealing with a nonequilibrium system.

Especially in the OTE system, we may conclude that sliding occurred at a well-defined slip plane. This is similar to plastic deformation of solids which is attributed to slipping at grain boundaries.<sup>4</sup> In view of the similar phenomenology, one is tempted to apply this idea to squalane and to look for the grain boundaries in this system. First one has to note that mica has a high-energy surface and certainly interacts with squalane molecules rather strongly. Assuming that the smoothness of the mica walls and their well-defined separation induce some kind of orientation of the molecules prompts one to expect layering, either in the sense of one

compact layer of squalane between the walls, or of molecules adsorbed at the opposing walls. In either case one would have the possibility of a slippage plane parallel to the mica walls, either at the walls or somewhere within the film. It is then plausible to expect that the weakest link will break first.

In other experiments with nonpolar hydrocarbon liquids confined between OTE monolayers, which are only partially wet by organic liquids because the surface energy of OTE is so low, we also observed qualitatively similar behavior. The position of the slip plane should be a function of the surface energy. In the present experiments with mica, slip may occur within the thin film; squalane layers may slip against one another. For solids of low surface energy, such as OTE, slip may take place at the solid wall. The slip behavior inferred here thus is seen to be a general effect—not depending on the presence of a high-energy surface.

It is worthwhile to compare our results with phenomenologically similar behavior of other systems. An analogous transition from an elastic state at rest to a sliding or flowing state was observed in granular media<sup>53,54</sup> and in concentrated suspensions.<sup>55–59</sup> Earthquake models also yield somewhat similar effects.<sup>60,61</sup> The instabilities of a sandpile especially resemble the present findings in respect that an avalanche down a sandpile is characterized by a well localized plane above which all the motion takes place. It looks like a sheet of sand sliding down the pile.<sup>53,54</sup> However, we do not mean to suggest that our systems show features of self-organized criticality that have been sometimes inferred in sandpiles.

Similarly, in concentrated suspensions, yielding and the existing of shear bands are reported. Computer simulations of ordered block copolymer systems under oscillatory shear showed responding waveforms very similar to the ones found in this study.<sup>42</sup> In block copolymers, slipping along a plane within the sample was directly observed and the waveforms can be confidently attributed to slippage.

The independence (or weak dependence) of the frictional force on sliding velocity can be attributed to two possible effects. Either the strength of interaction across the interface between the two OTE monolayers (or across the weakest link in the squalane case) became increasingly weaker as the sliding velocity increased *or* once the molecules were pulled a little out of their attractive wells there was no additional barrier stopping them from moving laterally. It was, however, not necessary to separate the molecules at the interface completely and thus the frictional force was not directly related to the interfacial work of adhesion. Even at small negative normal loads the surfaces did not separate in the sliding state. We can speculate that the molecules at the interface where slip occurred were dragged partially above their potential minima and moved along potential “valleys” surrounded by potential “mountains.” Even if the molecules were momentarily trapped in their potential wells they may have had enough kinetic energy to leave them again. This idea is a little reminiscent of the proposed superlubric state<sup>16</sup> where no frictional force is expected if two crystalline but incommensurate bodies slide past each other. In our case we have friction because we need to pull the molecules out of their potential wells first.

The increase in dissipative stress at the highest velocities might be speculatively explained along the same lines. Moving the top surface too fast might not allow one to find the path along the valley; the molecules would have to “climb” over the mountains. The upturn in stress might thus be due to the onset of turbulences within the film.

The elastic component of the shear stress decreased with increasing deflection amplitude. Possibly the elastic links between the moving parts were destroyed more and more, giving support to the idea of similarity to plastic deformation.

The reduction of the force needed to separate the OTE surfaces in the sliding state can be interpreted in the following way. Shear might induce normal forces which tended to separate the two monolayers. The actual increase in film thickness might be very small, too small to measure with our device. The force to pull the surfaces apart would then be reduced by the thickness dependence of the force-distance profile. The adhesive energy is reduced because the surfaces are not in closest contact anymore. This shear effect depends on the amplitude of deflection (probably on velocity) as is shown by ramping the amplitude for OTE layers under negative load. However, in addition to this effect just discussed, we may also expect high velocities to alter the structure of the confined system, thereby altering the form of the force-distance profile itself.

Increasing the load on the system certainly increased the shear forces. It is however, not clear, at small loads, if the shear stress increased too, as the uncertainty for measuring the area was comparable to the area we measured. We interpret the results for squalane especially at low loads mostly as an effect of an increase in the area. We can be more confident of the relative effect at larger loads. According to JKR theory the diameter of the contact area cubed is proportional to load. In the case of OTE we expect a small increase in contact area if we add 2 mN external load. Consequently the increase in shear force cannot be completely attributed to an increase in area. One might assume, under applied load conditions, that local rearrangements of molecules (increased order) might result in a more intimate contact or some interdigitation of the molecules which would resist shear more efficiently.

In summary, comparing the two systems investigated here we are inclined to attribute the transition from static to dynamic friction, from a highly elastic to mostly dissipative state, to a process similar to plastic deformation. The OTE system shows that sliding along an interfacial plane exhibits essentially the same features as squalane. This behavior of liquids under extremely large confinement contrasts with the perturbed liquid-like response observed for thicker films and at lesser normal pressures.

## ACKNOWLEDGMENTS

We thank Dr. Carl Kessel for advice concerning the OTE monolayer formation. This work was supported by taxpayers of the United States via grants from the National Science Foundation, Tribology Program, NSF-MSM-92-02143 (to A. L. D.) and the Air Force, Grant No. AFOSR-URI-F49620-93-1-02-41 (to G. R.). We also thank the Exxon Corporation for financial support.

- <sup>1</sup> *Fundamentals of Friction*, edited by I. L. Singer and H. M. Pollock (Kluwer Academic, Dordrecht, 1992).
- <sup>2</sup> D. Tabor, in *Microscopic Aspects of Adhesion and Lubrication*, edited by J. M. Georges (Elsevier, New York, 1982), p. 651.
- <sup>3</sup> F. P. Bowden and D. Tabor, *The Friction and Lubrication of Solids*, Part II (Clarendon, Oxford, 1964).
- <sup>4</sup> F. P. Bowden and D. Tabor, *Friction: An Introduction to Tribology* (Anchor/Doubleday, New York, 1973).
- <sup>5</sup> J. Skinner and N. Gane, *J. Phys. D* **5**, 2087 (1972).
- <sup>6</sup> M. J. Sutcliffe, S. R. Taylor, and A. Cameron, *Wear* **51**, 181 (1978).
- <sup>7</sup> J. N. Israelachvili, in Ref. 1, p. 351.
- <sup>8</sup> B. J. Briscoe and D. C. B. Evans, *Proc. R. Soc. London Ser. A* **380**, 389 (1982).
- <sup>9</sup> R. M. Overney, E. Meyer, J. Frommer, D. Brodbeck, R. Lüthi, L. Howald, H. J. Güntheradt, M. Fujihira, H. Takano, and Y. Gotoh, *Nature* **359**, 133 (1992).
- <sup>10</sup> C. M. Mate, G. M. McClelland, R. Erlandsson, and S. Chiang, *Phys. Rev. Lett.* **59**, 1942 (1987).
- <sup>11</sup> B. N. J. Persson, *Phys. Rev. Lett.* **71**, 1212 (1993).
- <sup>12</sup> J. N. Glosli and G. M. McClelland, *Phys. Rev. Lett.* **70**, 1960 (1993).
- <sup>13</sup> J. B. Sokoloff, *Wear* **167**, 59 (1993); *Phys. Rev. B* **42**, 760 (1990).
- <sup>14</sup> W. Zhong and D. Tománek, *Phys. Rev. Lett.* **64**, 3054 (1990).
- <sup>15</sup> J. A. Harrison, C. T. Carter, R. J. Colton, and D. W. Brenner, *MRS Bull.* **18**, 50 (1993).
- <sup>16</sup> K. Shinjo and M. Hirano, *Surf. Sci.* **283**, 473 (1993); M. Hirano, K. Shinjo, R. Kaneko, and Y. Murata, *Phys. Rev. Lett.* **67**, 2642 (1991).
- <sup>17</sup> M. Schoen, C. L. Rhykerd, D. J. Diestler, and J. H. Cushman, *Science* **245**, 1223 (1989).
- <sup>18</sup> P. A. Thompson and M. O. Robbins, *Science* **250**, 792 (1990); *Phys. Rev. A* **41**, 6830 (1990).
- <sup>19</sup> P. A. Thompson, G. S. Grest, and M. O. Robbins, *Phys. Rev. Lett.* **68**, 3448 (1992).
- <sup>20</sup> J. N. Israelachvili and P. M. McGuiggan, *Science* **241**, 795 (1988).
- <sup>21</sup> J. Van Alsten and S. Granick, *Phys. Rev. Lett.* **62**, 463 (1988).
- <sup>22</sup> M. L. Gee, P. M. McGuiggan, J. N. Israelachvili, and A. M. Homola, *J. Chem. Phys.* **93**, 1895 (1990).
- <sup>23</sup> J. Van Alsten and S. Granick, *Langmuir* **6**, 876 (1990).
- <sup>24</sup> S. Granick, *Science* **253**, 1374 (1991); H.-W. Hu and S. Granick, *Science* **258**, 1339 (1992).
- <sup>25</sup> H. Yoshizawa, P. M. McGuiggan, and J. N. Israelachvili, *Science* **259**, 1305 (1993).
- <sup>26</sup> H. Yoshizawa, Y.-I. Chen, and J. N. Israelachvili, *J. Phys. Chem.* **97**, 4128 (1993).
- <sup>27</sup> H. Yoshizawa and J. N. Israelachvili, *J. Phys. Chem.* **97**, 11,300 (1993).
- <sup>28</sup> J. Van Alsten and S. Granick, *Tribology Trans.* **32**, 246 (1989).
- <sup>29</sup> H.-W. Hu, G. A. Carson, and S. Granick, *Phys. Rev. Lett.* **66**, 2758 (1991).
- <sup>30</sup> C. M. Mate, *Phys. Rev. Lett.* **68**, 3323 (1992).
- <sup>31</sup> J. Krim, D. H. Solina, and R. Chiarello, *Phys. Rev. Lett.* **66**, 181 (1991).
- <sup>32</sup> J. Krim and R. Chiarello, *J. Vac. Sci. Technol. A* **9**, 2599 (1991).
- <sup>33</sup> M. J. Chaudhury and M. J. Owen, *J. Phys. Chem.* **97**, 5722 (1993).
- <sup>34</sup> G. Reiter, A. L. Demirel, and S. Granick, *Science* **263**, 1741 (1994).
- <sup>35</sup> J. Peachey, J. Van Alsten, and S. Granick, *Rev. Sci. Instrum.* **62**, 463 (1991).
- <sup>36</sup> C. R. Kessel and S. Granick, *Langmuir* **7**, 532 (1991).
- <sup>37</sup> J. Peanasky, H. Schneider, S. Granick, and C. R. Kessel (to be published).
- <sup>38</sup> N. Camillone III, C. E. D. Chidsey, P. Eisenberger, P. Fenter, J. Li, K. S. Liang, G. Y. Liu, and G. Scoles, *J. Chem. Phys.* **99**, 744 (1993).
- <sup>39</sup> In those experiments the driver and the liquid can be represented by a mechanical model of two springs in series, i.e., the force acting on the liquid is the same as on the driving spring. However, the deformation of the two springs is different.
- <sup>40</sup> S. Onogi, T. Masuda, and T. Matsumoto, *Trans. Soc. Rheol.* **14**, 275 (1970).
- <sup>41</sup> A. J. Giacomini and J. G. Oakley, *Rheol. Acta* **32**, 328 (1993).
- <sup>42</sup> T. Ohta, Y. Enomoto, J. L. Harden, and M. Doi, *Macromolecules* **26**, 4928 (1993).
- <sup>43</sup> A. J. Giacomini, R. S. Jeyaseelan, T. Samurkas, and J. M. Dealy, *J. Rheol.* **37**, 811 (1993).
- <sup>44</sup> J. D. Ferry, *Viscoelastic Properties of Polymers*, 3rd ed. (Wiley, New York, 1980).
- <sup>45</sup> This ratio can be interpreted as strain, however, it is questionable if the film can be treated as an isotropic continuum in order to justify this assumption. Due to attractive forces molecules close to the mica surfaces might behave differently than molecules in the center of the film.
- <sup>46</sup> A. L. Demirel, J. Peanasky, L. Cai, and S. Granick (to be published).
- <sup>47</sup> The deformation of the confined film ( $x_{0,crit}$ ) at  $\sigma_{0,crit}$  was of the order of 1 nm. This value is somewhat uncertain as it depends sensitively on the correction for deformation of the device (mostly within the glue layers).  $x_{0,crit}$  can vary by as much as a factor of 2.
- <sup>48</sup> As it is not customary to distinguish between the elastic and dissipative contributions to a sliding force, we have followed common practice and defined the friction coefficient in terms of the acting force. From a physical point of view one might wish to consider only the dissipative part, as friction is related to loss of energy. In any case, the elastic contribution is lower than the dissipative part (note that the forces in Fig. 13 are plotted on logarithmic scales). Consequently the choice of definition makes little actual difference in this case.
- <sup>49</sup> K. L. Johnson, K. Kendall, and A. D. Roberts, *Proc. R. Soc. London Ser. A* **324**, 301 (1971).
- <sup>50</sup> L. Bragg and J. F. Nye, *Proc. R. Soc. London Ser. A* **190**, 474 (1947).
- <sup>51</sup> W.-J. Ma, J. R. Banavar, and J. Koplik, *J. Chem. Phys.* **97**, 485 (1992).
- <sup>52</sup> M. W. Ribarsky and U. Landmann, *J. Chem. Phys.* **97**, 1937 (1992); T. K. Xia, J. Ouyang, M. W. Ribarsky, and U. Landmann, *Phys. Rev. Lett.* **69**, 1967 (1992).
- <sup>53</sup> H. M. Jaeger, C.-H. Liu, S. R. Nagel, and T. A. Witten, *Europhys. Lett.* **11**, 619 (1990); H. M. Jaeger and S. R. Nagel, *Science* **255**, 1523 (1992).
- <sup>54</sup> P. A. Thompson and G. S. Grest, *Phys. Rev. Lett.* **67**, 1751 (1991).
- <sup>55</sup> R. L. Hoffman, *Trans. Soc. Rheol.* **16**, 155 (1972).
- <sup>56</sup> B. E. Rodriguez, M. S. Wolfe, and E. W. Kaler, *Langmuir* **9**, 12 (1993).
- <sup>57</sup> A. Bradbury, J. W. Goodwin, and R. W. Hughes, *Langmuir* **8**, 2863 (1992).
- <sup>58</sup> L. B. Chen, C. F. Zukoski, B. J. Ackerson, H. J. M. Hanley, G. C. Straty, J. Barker, and C. J. Glinka, *Phys. Rev. Lett.* **69**, 688 (1992); L. B. Chen and C. F. Zukoski, *J. Chem. Soc. Faraday Trans.* **86**, 2629 (1990).
- <sup>59</sup> B. Cabane (private communication).
- <sup>60</sup> J. M. Carlson and J. S. Langer, *Phys. Rev. Lett.* **62**, 2632 (1989).
- <sup>61</sup> M. de Sousa Vieira, G. L. Vasconcelos, and S. R. Nagel, *Phys. Rev. E* **47**, R2221 (1993).